

Nonpolar resistive switching in the Pt/MgO/Pt nonvolatile memory device

Cite as: Appl. Phys. Lett. **96**, 193505 (2010); <https://doi.org/10.1063/1.3429024>

Submitted: 29 December 2009 • Accepted: 22 April 2010 • Published Online: 13 May 2010

Hsin-Hung Huang, Wen-Chieh Shih and Chih-Huang Lai



View Online



Export Citation

ARTICLES YOU MAY BE INTERESTED IN

[Conduction mechanism of resistive switching films in MgO memory devices](#)

Journal of Applied Physics **111**, 094104 (2012); <https://doi.org/10.1063/1.4712628>

[Resistive switching phenomena: A review of statistical physics approaches](#)

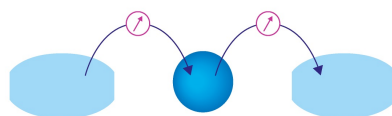
Applied Physics Reviews **2**, 031303 (2015); <https://doi.org/10.1063/1.4929512>

[Resistive switching mechanism of TiO₂ thin films grown by atomic-layer deposition](#)

Journal of Applied Physics **98**, 033715 (2005); <https://doi.org/10.1063/1.2001146>

Webinar

Interfaces: how they make
or break a nanodevice



March 29th – Register now



Zurich
Instruments

AIP
Publishing

Nonpolar resistive switching in the Pt/MgO/Pt nonvolatile memory device

Hsin-Hung Huang, Wen-Chieh Shih, and Chih-Huang Lai^{a)}

Department of Materials Science and Engineering, National Tsing Hua University, Hsinchu 30013, Taiwan

(Received 29 December 2009; accepted 22 April 2010; published online 13 May 2010)

Nonpolar resistive switching (RS), which is the coexistence of unipolar and bipolar RS characteristics, in the Pt/MgO/Pt memory device with the nonforming nature is demonstrated. The nonforming nature is ascribed to the relatively high defect density of the MgO film deposited by using the ion beam sputtering in Ar atmosphere. The results of Auger electron spectroscopy and x-ray photoelectron spectroscopy analyses combining with the temperature dependence of resistance suggest that metallic Mg filaments are formed in the low resistance state. The voltage-polarity-independent RESET process implies that filaments may be ruptured by local Joule heating, leading to nonpolar characteristics. © 2010 American Institute of Physics.

[doi:10.1063/1.3429024]

Resistive switching (RS) phenomena have been extensively investigated for the development of next-generation nonvolatile resistive random access memory (RRAM) devices.¹ Promising performances of long endurance ($>10^8$ cycles) and fast programming speed (<50 ns) have also been demonstrated in the nanoscale amorphous-Si-based RRAM device recently.² However, the underlying mechanism of RS behavior is still not yet clearly understood, and various models have been proposed, such as conducting filaments composed of metallic atoms³ or oxygen vacancies,⁴ Schottky emission,⁵ and trap-controlled space-charge-limited current.⁶

In recent years, different RS phenomena have been reported in CoFeB/MgO/CoFeB magnetic tunneling junctions (MTJs), including unipolar⁷ and bipolar RS characteristics.^{8,9} Different from other RRAM systems, the electronic transport of MgO-based MTJs is dominated by the quantum tunneling effect of $3d$ electrons of ferromagnetic layers through an ultrathin MgO tunneling barrier of tens of angstrom, which can still occur even in the high resistance state (HRS) of MTJ-based RRAMs. Furthermore, in MgO-based MTJs, to achieve a high tunneling magnetoresistance ratio, a postannealing process is typically performed to obtain the crystallization of (002) CoFeB/MgO/CoFeB.¹⁰ However, the ultrathin MgO tunneling barrier may be significantly influenced by the diffusion of B atoms and by the formation of BO_x complexes induced during the postannealing process,¹¹ which may complicate the study on the origin of RS behavior in MgO-based RRAMs.

In this paper, MgO memory devices with relatively thick MgO films and Pt electrodes were fabricated to study the underlying origin of RS behavior. Different from conventional binary-oxide RRAMs, no forming process is required to initiate RS behavior in our MgO memory device. Moreover, in contrast to RS behavior reported in MgO-MTJ-based RRAMs,⁷⁻⁹ nonpolar RS behavior, which has also been observed recently in other systems,¹²⁻¹⁵ is revealed in our MgO memory device.

MgO films of 60 nm were deposited on Si/SiO₂/Ti 10/Pt 10 (nm) substrates by using the ion beam sputtering with Ar bombarding on a commercial MgO target at room

temperature. The ion beam voltage and current were 750 V and 30 mA, respectively. To perform RS measurements, circle-shaped 60 nm thick Pt top electrodes of 200 μm in diameter were deposited on the blanket MgO film with a shadow mask. The MgO memory device was postannealed under a vacuum level of 1×10^{-5} Torr at 300 °C for 2 h. RS characteristics were investigated by using the Keithley 4200 semiconductor characterization system.

The typical current-voltage curves of the MgO memory device, as shown in Fig. 1, exhibit nonpolar RS behavior, which is the coexistence of unipolar [Figs. 1(a) and 1(d)] and bipolar [Figs. 1(b) and 1(c)] RS characteristics in one device. When a positive or negative dc voltage sweep with a compliance current of 1 mA applied to the MgO memory device, as shown in the open-square curves of Figs. 1(a)–1(d), a SET-process-induced resistance transition from the HRS to the low resistance state (LRS) is revealed by an abrupt increase in the current at the SET voltage. On the other hand, the RESET process, which is defined as the resistance state switches from the LRS to the HRS revealed by an abrupt decrease in the current, can be achieved by resweeping a

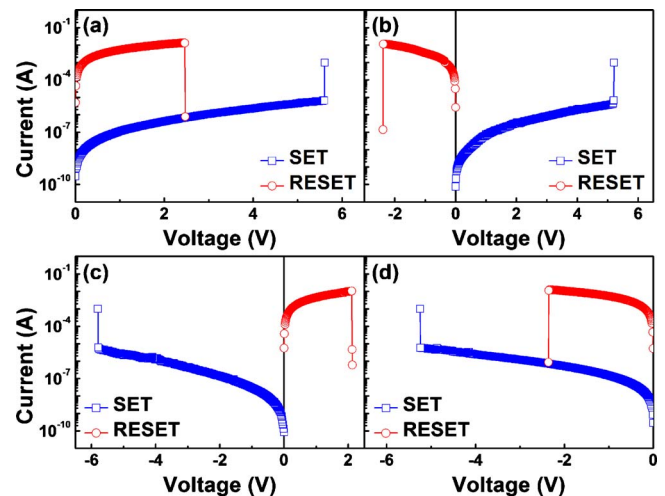


FIG. 1. (Color online) Nonpolar RS behavior, the coexistence of [(a) and (d)] unipolar and [(b) and (c)] bipolar RS characteristics, is observed in the MgO memory device. The SET-RESET processes can be achieved by (a) positive-positive, (b) positive-negative, (c) negative-positive, and (d) negative-negative voltage polarities.

^{a)}Electronic mail: chlai@mx.nthu.edu.tw.

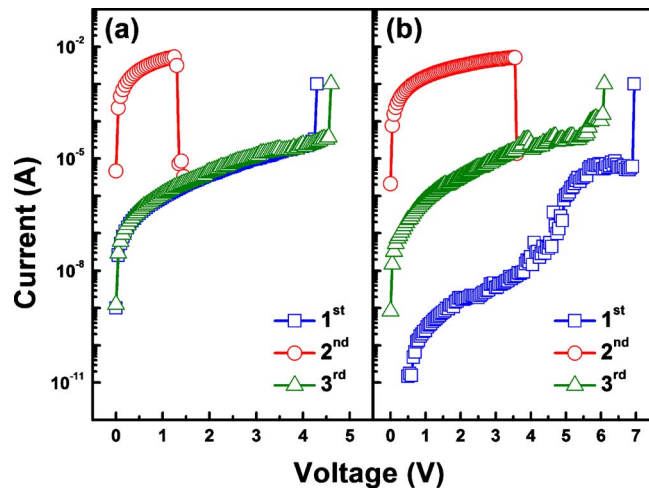


FIG. 2. (Color online) The first three dc voltage sweeps applied to the as-fabricated MgO memory devices with the MgO films deposited in (a) the Ar atmosphere, showing the nonforming nature; and in (b) the Ar+O₂ 20% atmosphere, showing the requirement of the forming process.

positive or negative dc voltage to the RESET voltage, as shown in the open-circle curves of Figs. 1(a)–1(d). These results clearly demonstrate the voltage-polarity-independent nonpolar characteristic of the MgO memory device, that is, the SET-RESET processes can be achieved by positive-positive [Fig. 1(a)], positive-negative [Fig. 1(b)], negative-positive [Fig. 1(c)], and negative-negative [Fig. 1(d)] voltage polarities. The resistance ratio of the HRS to the LRS is in the order of 10^5 , showing no significant degradation during 100 switching cycles. The resistance values of both states revealed no significant fluctuation (less than 5%) at 85 °C over 2×10^4 s. In addition, the LRS resistance of the MgO memory device is insensitive to the top electrode area ranging from 200 to 500 μm in diameter, implying the nonuniform current distribution through localized conducting filaments in the MgO film (not shown here).

In conventional binary-oxide RRAMs, RS behavior is initiated by a forming process, which establishes the connection between percolated conducting filaments (mainly related to defects in oxides) and provides the stimulation of an electric stress with a significantly larger electric field than that required for the SET process. Furthermore, the forming process induces additional defects, which may be irreversible; therefore, the resistance of the initial resistance state (IRS) is larger than the HRS resistance.¹⁶ However, as shown in Fig. 2(a), the first three dc voltage sweeps applied to the as-fabricated MgO memory device show that the SET voltage of the first voltage sweep is similar to that of the third voltage sweep, and the difference between the IRS resistance (obtained from the first voltage sweep) and the HRS resistance (obtained from the third voltage sweep) is insignificant. These results indicate the nonforming nature of the MgO memory device. Since the MgO film was deposited by using the ion beam sputtering in Ar atmosphere, a relatively high density of defects may be created during the deposition.¹⁷ Therefore, as the first voltage sweep was applied to the as-fabricated MgO memory device, the ratio of the induced additional defects to the preexisting defects may not be as significant as that of other RRAM systems during the forming process. Due to the existence of many preexisting defects in the MgO film, no forming process is observed. Furthermore,

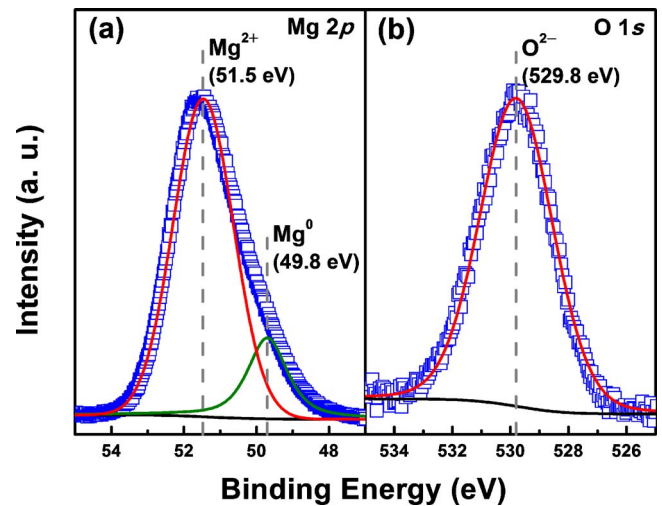


FIG. 3. (Color online) The XPS spectra of the MgO film of (a) Mg 2p, indicating the coexistence of Mg²⁺ in MgO (Mg²⁺ at 51.5 eV) in majority and metallic Mg (Mg⁰ at 49.8 eV) in minority; and of (b) O 1s, indicating the existence of lattice oxygen ions (O²⁻ at 529.8 eV). The solid lines represent the fitted spectra.

the SET voltage of 6 V of the MgO memory device, corresponding to an electric field of 1 MV/cm, is much smaller than that of MgO-MTJ-based RRAMs (4–13 MV/cm) (Refs. 7–9) and the soft breakdown field of 5–6 MV/cm of the 20 nm thick MgO film.¹⁸ This result may be also ascribed to the relatively high defect density in the MgO film. To further elucidate the nonforming nature of the MgO film, we introduced Ar+O₂ 20% atmosphere during the deposition of the MgO film (the MgO:O film). The first three dc voltage sweeps applied to the as-fabricated MgO memory device with the MgO:O film, as shown in Fig. 2(b), indicate that the SET voltage of the first voltage sweep is larger than that of the third voltage sweep, and the IRS resistance (obtained from the first voltage sweep) is significantly larger than the HRS resistance (obtained from the third voltage sweep), revealing the requirement of the forming process. These results indicate that the Ar+O₂ 20% atmosphere introduced during the deposition may reduce the number of defects in the MgO film; therefore, a forming process is required to initiate RS behavior.

To clarify the type of defects in the MgO film, we performed the x-ray photoelectron spectroscopy (XPS) analysis with the synchrotron radiation light source to investigate chemical states of Mg and oxygen. The Mg 2p spectrum, as shown in Fig. 3(a), indicates the coexistence of Mg²⁺ in MgO (Mg²⁺ at 51.5 eV) in majority and metallic Mg (Mg⁰ at 49.8 eV) in minority. On the other hand, the O 1s spectrum, as shown in Fig. 3(b), indicates the existence of lattice oxygen ions (O²⁻ at 529.8 eV). Furthermore, no nonlattice oxygen ions, which were reported to be responsible for bipolar RS behavior with filaments composed of oxygen vacancies in the ZnO film,⁴ are observed in the O 1s spectrum. These results imply that metallic Mg may play a crucial role in RS behavior of the MgO memory device.

To further elucidate the physical origin of filaments in the MgO film, we measured the temperature dependence of the LRS resistance at the temperature range of 25–120 °C (298–393 K). It should be mentioned that RS behavior was observable at the whole temperature range. The MgO memory device was first switched to the LRS, and then the

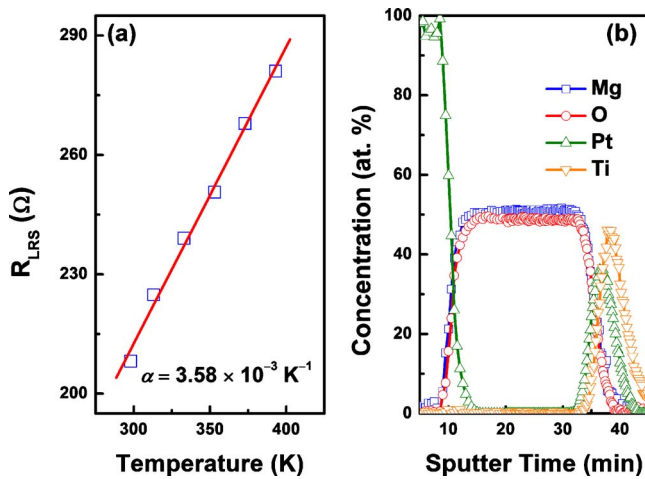


FIG. 4. (Color online) (a) The temperature dependence of the LRS resistance measured with 100 mV. The solid line represents the linear fit. (b) The AES compositional depth profile of the MgO memory device in the LRS after 100 switching cycles.

LRS resistance was measured at various measuring temperatures. Figure 4(a) shows the temperature dependence of the LRS resistance, which can be linear-fitted with a positive slope, indicating a typical characteristic of the electronic transport in metals. The temperature dependence of the metallic resistance can be expressed as $R(T) = R_0[1 + \alpha(T - T_0)]$, where R_0 is the resistance at the reference temperature T_0 , and α is the temperature coefficient of resistance. By choosing T_0 as 298 K, α of the MgO memory device in the LRS can be calculated as $3.58 \times 10^{-3} \text{ K}^{-1}$, which corresponds well with the experimental result of the Mg film with α of $3.25 \times 10^{-3} \text{ K}^{-1}$ at T_0 of 293 K.¹⁹ The resistance change contributed by Pt and Ti electrodes with the increasing temperature is much smaller than the measured value, and α values of Pt and Ti are distinct from the calculated value. In addition, we performed the compositional depth profile of the MgO memory device in the LRS after 100 switching cycles by using the Auger electron spectroscopy (AES). A single crystal MgO substrate was used to calibrate the AES compositional depth profile of the MgO film. The difference between the atomic concentration of Mg and oxygen is observed, as shown in Fig. 4(b), revealing that the content of Mg is slightly but distinguishably higher than that of oxygen in the MgO film. This result implies that the MgO film is nonstoichiometric. Furthermore, the AES compositional depth profile of the MgO memory device in the LRS after 100 switching cycles shows no obvious difference from that of the as-fabricated MgO memory device (not shown here), indicating that there is no significant diffusion or electromigration of Pt and Ti atoms into the MgO film. Therefore, the AES and XPS results combining with the temperature dependence of the LRS resistance suggest that filaments in the MgO film are mainly composed of metallic Mg.

According to the aforementioned experimental results, nonpolar RS behavior with the nonforming nature in the MgO memory device can be realized as follows. Since the relatively high density of defects in the MgO film, no forming process is required to initiate RS behavior. However, the number of defects in the MgO film can be reduced by the introduction of Ar+O₂ 20% atmosphere during the deposition of the MgO film (the MgO:O film), demonstrating the

stoichiometry controlled forming process. During the SET process, the formation of metallic Mg filaments in the MgO film is triggered by an electric stress; therefore, the MgO memory device is switched from the HRS to the LRS. For the RESET process, since it can be achieved by both positive and negative voltage polarities regardless of the voltage polarity of the SET process, we suggest that local Joule heating may assist the rupture of filaments to switch the MgO memory device from the LRS to the HRS.

In summary, nonpolar RS behavior in the Pt/MgO/Pt memory device with the nonforming nature is demonstrated. RS behavior for the SET process is attributed to the formation of metallic Mg filaments, which is well supported by the AES and XPS results combining with the temperature dependence of the LRS resistance. The voltage-polarity-independent RESET process implies that local Joule heating may assist the rupture of filaments, leading to nonpolar characteristics.

The authors gratefully acknowledge C. H. Chen and H. W. Shiu of the 09A1 beamline of the National Synchrotron Radiation Research Center in Taiwan for fruitful discussions and technical support. This work was partially supported by the Ministry of Economic Affairs of Republic of China under the Grant No. 98-EC-17-A-08-S1-006 and the National Science Council of Republic of China under the Grant No. 98-2622-E-007-003.

¹R. Waser and M. Aono, *Nat. Mater.* **6**, 833 (2007).

²K. H. Kim, S. H. Jo, S. Gaba, and W. Lu, *Appl. Phys. Lett.* **96**, 053106 (2010).

³M. J. Lee, S. Han, S. H. Jeon, B. H. Park, B. S. Kang, S. E. Ahn, K. H. Kim, C. B. Lee, C. J. Kim, I. K. Yoo, D. H. Seo, X. S. Li, J. B. Park, J. H. Lee, and Y. Park, *Nano Lett.* **9**, 1476 (2009).

⁴N. Xu, L. Liu, X. Sun, X. Liu, D. Han, Y. Wang, R. Han, J. Kang, and B. Yu, *Appl. Phys. Lett.* **92**, 232112 (2008).

⁵T. Fujii, M. Kawasaki, A. Sawa, H. Akoh, Y. Kawazoe, and Y. Tokura, *Appl. Phys. Lett.* **86**, 012107 (2005).

⁶Y. C. Yang, F. Pan, Q. Liu, M. Liu, and F. Zeng, *Nano Lett.* **9**, 1636 (2009).

⁷C. Yoshida, M. Kurasawa, Y. M. Lee, M. Aoki, and Y. Sugiyama, *Appl. Phys. Lett.* **92**, 113508 (2008).

⁸J. M. Teixeira, J. Ventura, R. Fermento, J. P. Araujo, J. B. Sousa, P. Wisniowski, and P. P. Freitas, *J. Phys. D* **42**, 105407 (2009).

⁹P. Krzysteczko, G. Reiss, and A. Thomas, *Appl. Phys. Lett.* **95**, 112508 (2009).

¹⁰D. D. Djayaprawira, K. Tsunekawa, M. Nagai, H. Maehara, S. Yamagata, N. Watanabe, S. Yuasa, Y. Suzuki, and K. Ando, *Appl. Phys. Lett.* **86**, 092502 (2005).

¹¹J. J. Cha, J. C. Read, R. A. Buhrman, and D. A. Muller, *Appl. Phys. Lett.* **91**, 062516 (2007).

¹²C. C. Lin, C. Y. Lin, M. H. Lin, C. H. Lin, and T. Y. Tseng, *IEEE Trans. Electron Devices* **54**, 3146 (2007).

¹³C. Schindler, S. C. P. Thermanad, R. Waser, and M. N. Kozicki, *IEEE Trans. Electron Devices* **54**, 2762 (2007).

¹⁴W. Guan, M. Liu, S. Long, Q. Liu, and W. Wang, *Appl. Phys. Lett.* **93**, 223506 (2008).

¹⁵I. H. Inoue, S. Yasuda, H. Akinaga, and H. Takagi, *Phys. Rev. B* **77**, 035105 (2008).

¹⁶S. C. Chae, J. S. Lee, S. Kim, S. B. Lee, S. H. Chang, C. Liu, B. Kahng, H. Shin, D. W. Kim, C. U. Jung, S. Seo, M. J. Lee, and T. W. Noh, *Adv. Mater.* **20**, 1154 (2008).

¹⁷H. H. Huang, C. A. Yang, P. H. Huang, C. H. Lai, T. S. Chin, H. E. Huang, H. Y. Bor, and R. T. Huang, *J. Appl. Phys.* **101**, 09H116 (2007).

¹⁸E. Miranda, E. O'Connor, K. Cherkaoui, S. Monaghan, R. Long, D. O'Connell, P. K. Hurley, G. Hughes, and P. Casey, *Appl. Phys. Lett.* **95**, 012901 (2009).

¹⁹P. Renucci, L. Gaudart, J. P. Petrakian, and D. Roux, *Thin Solid Films* **130**, 75 (1985).